Heliyon 10 (2024) e24401

Contents lists available at ScienceDirect

Heliyon

journal homepage: www.cell.com/heliyon

Research article

Eriodictyol inhibits the motility, angiogenesis and tumor growth of hepatocellular carcinoma via NLRP3 inflammasome inactivation

Wei Huang, Chenyang Wang, Hui Zhang *

Department of Hepatobiliary and Pancreatic Surgery, Third Xiangya Hospital, Central South University, Changsha, 410013 Hunan, China

ARTICLE INFO

Keywords:
Hepatocellular carcinoma
NLRP3
Eriodictyol
Metastasis

ABSTRACT

NLRP3 involves in the development of hepatocellular carcinoma (HCC). Eriodictyol has shown its inhibitory effect on HCC cell proliferation. However, the underlying mechanism of eriodictyol in HCC is still unclear. This study aimed to explore the effect of and mechanism of eriodictyol on HCC. In this study, compared with eriodictyol (0 μM) group, eriodictyol significantly suppressed HepG2 cells (eriodictyol of 25, 50 and 100 μM) and Huh-7 cells (eriodictyol of 50 and 100 μM) viability, invasion, tube formation, metastasis-related genes MMP3, MMP16 and angiogenesis regulator VEGFA expressions with IC_{50} of 45.63 μM and 78.26 μM *in vitro*, respectively. Besides, eriodictyol significantly repressed NLRP3 expression, and reduced the protein levels of NLRP3 inflammasome-related proteins, adapter protein ASC, caspase-1, interleukin (IL)-18, and IL-1β in HepG2 (eriodictyol of 25, 50 and 100 μM) and Huh-7 cells (eriodictyol of 50 and 100 μM), respectively. Meanwhile, compared with control group, NLRP3 overexpression reversed the anti-metastatic effects of 100 μM eriodictyol on HCC cells invasion, tube formation, and metastasis-related genes MMP3, MMP16 and angiogenesis regulator VEGFA expressions, whereas NLRP3 knockdown enhanced the anti-metastatic effects of 100 μM eriodictyol on HCC cells. *In vivo*, compared with control group, eriodictyol significantly reduced the tumor growth, liver damage, inhibited the activation of NLRP3 inflammasome, and improved liver function, whereas NLRP3 overexpressing neutralized the anti-tumor effects of eriodictyol and degraded liver function. Hence, eriodictyol inhibited HCC cell viability, motility, angiogenesis and tumor growth via NLRP3 inflammasome inactivation both *in vitro* and *in vivo*.

1. Introduction

As one of the most common and aggressive tumors, hepatocellular carcinoma (HCC) is the sixth leading cause of mortality in cancer in the world [1]. In China, hepatitis B virus can lead to a high infection rate of HCC, so attention should be paid to the surveillance and treatment of HCC [2]. Excitingly, there has been development in clinical surveillance and therapy for HCC. However, the prognosis of HCC remains unsatisfactory due to the frequency of metastasis and high recurrence of the primary tumor [3]. Therefore, developing potential prognosis biomarkers and effective therapeutic strategies for patients with HCC are urgently needed.

* Corresponding author. Third Xiangya Hospital, Central South University, 138 Tongzipo Road, Yuelu District, Changsha City, Hunan Province, China.
E-mail address: zhanhuixy@126.com (H. Zhang).

https://doi.org/10.1016/j.heliyon.2024.e24401
Received 7 June 2023; Received in revised form 14 December 2023; Accepted 8 January 2024
Available online 20 January 2024

Recently, natural herbs play an irreplaceable role in modern antitumor drug discovery, owing to their high efficiency and limited toxicity [4]. Eriodictyol is a flavone subclass of flavonoids extracted from vegetables, fruits, and several medicinal plants [5–7]. Eriodictyol has been shown to have anti-inflammatory, antioxidant, and neuroprotective effects [8–10]. Importantly, the anti-tumor effects of eriodictyol in some malignancies were also reported. Tang et al. showed eriodictyol repressed CNE1 nasopharyngeal cancer cell growth, migration, and invasion by targeting MEK/ERK signaling [11]. Eriodictyol played an anticancer role in the A549 lung cancer cells through facilitating cell cycle arrest and apoptosis and inhibiting the m-TOR/PI3K/Akt pathway [12]. Eriodictyol effectively inhibited glioma cell growth and metastasis and facilitated cell apoptosis via restraining PI3K/Akt/NF-kB pathway [13]. Although eriodictyol could repress the proliferation of liver cancer cell HepG2 [13], the underlying mechanism has not been revealed. Furthermore, the functional effect of eriodictyol on HCC cell metastasis is unreported.

The NOD-like receptor pyrin domain-containing 3 (NLRP3) inflammasome is a critical component of the innate immune system and can respond to microbial infection and cell damage [14]. NLRP3 activation recruits procaspase-1 and ASC to form NLRP3 inflammasome, while NLRP3 inflammasome activates procaspase-1. Activation of caspase-1 can pre-process pro-IL-18 and pro-IL-1β into mature IL-18 and IL-1β [15]. It has been shown that NLRP3 inflammasome involves in the development of several cancers, most of which were focused on proliferation, metastasis, angiogenesis, survival, and immunosuppression. For instance, NLRP3 was overexpressed in colorectal cancer and promoted the growth and metastasis via activating the Epithelial-Mesenchymal Transition (EMT) program [16]. Activation of NLRP3 inflammasome facilitated tumor progression and lung metastasis [17]. In laryngeal squamous cell carcinoma, patients with NLRP3 inflammasome activation, including overexpression of NLRP3, ASC, IL-18, and IL-1β, had an unfavorable prognosis [18]. NLRP3 inflammasome suppression in macrophages was associated with the suppression of the metastatic capacity of cancer cells [19]. Furthermore, repression of NLRP3 inflammasome activation inhibited HCC viability, growth and metastasis. Li et al. demonstrated that anisodamine restrained the viability and facilitated the apoptosis of HCC cells by blocking NLRP3 inflammasome activation [20]. Similarly, Fan et al. reported that luteoloside exerted an inhibitory role on HCC cell growth and metastasis via suppression of NLRP3 inflammasome [21]. IRAK1 knockdown restrained HCC malignant progression through inhibition of MAPKs/NLRP3/IL-1β pathway activation [22]. However, whether NLRP3 inflammasome was involved in the treatment of eriodictyol in HCC is not clear.

In this study, we demonstrated that eriodictyol was a potent agent against HCC cells *in vitro* and *in vivo*, and NLRP3 inflammasome might participate in the signaling of eriodictyol-induced inhibition of HCC cell metastasis. Collectively, our study expounded the underlying mechanism of eriodictyol in HCC metastasis repression.

2. Materials and methods

2.1. Cell culture and chemical reagents

HepG2 and Huh-7 cells were purchased from Procell (Wuhan, China). STR markers of HepG2 cells are as follows: CSF1PO (10, 11), D1S1656 (11, 12), D2S441 (11.3, 14), D2S1338 (19, 20), D3S1358 (15,16), D5S818 (11, 12), D7S820 (10), D8S1179 (15, 16), D10S1248 (13), D12S391 (21, 25), D13S317 (9, 13), D16S539 (12, 13), D18S51 (13, 14), D19S433 (15.2), D21S11 (29, 31), D22S1045 (16), DYS391 (12), FGA (22, 25), Penta D (9, 13), Penta E (15, 20), TH01 (9), TPOX (8, 9), vWA (17). STR markers of Huh-7 cells are as follows: CSF1PO (11), D1S1656 (16), D2S441 (12, 14), D2S1338 (19), D3S1358 (15), D5S818 (12), D6S1043 (13, 15), D7S820 (11), D8S1179 (14, 15), D10S1248 (16), D12S391 (20), D13S317 (10), D16S539 (10), D18S51 (15), D19S433 (13, 14), D21S11 (30), D22S1045 (17, 20), FGA (22, 23), Penta D (12), Penta E (11), TH01 (7), TPOX (8, 11), vWA (16, 18), which can be searched from https://www.cellosaurus.org. All cells were kept in DMEM with 10 % FBS and 100 U/mL penicillin/streptomycin (Gibco, Grand Island, NY, USA) under 5 % CO_2 as well as 37 °C condition. Eriodictyol was purchased from Sigma-Aldrich (MO, USA) with a purity ≥95.0 % by HPLC.

2.2. CCK-8 assay

The viability of HepG2 and Huh-7 was detected by CCK-8 kit (Beyotime, Shanghai, China). The cells (1×10^3 cells/well) were added to 96-well plates and cultured for 24 h at 37 °C. Then, different concentrations of eriodictyol (0, 12.5, 25, 50, 100, 200, 400, or 800 μM) were added into the medium, respectively. After 48 h, 10 μL CCK-8 solution was added into each well. Absorbance at 450 nm was recorded by a microplate reader (Bio-Rad, CA, USA).

2.3. Transwell assay to observe cell motility

HepG2 or Huh-7 cells (1×10^6 cells/well) mixed with the serum-free medium were seeded into the upper chamber of the transwell pretreated with Matrigel (Corning, NY, USA) and allowed to migrate toward DMEM containing 10 % FBS in the lower side of the chamber for 24 h. Eriodictyol (0, 25, 50, and 100 μM) were added to the upper chamber. Cells in the lower chamber were fixed in formaldehyde and stained with 0.1 % crystal violet for 20 min. The cells that migrated to the lower surface of the insert membrane were counted as invaded cells. The invaded cells were captured under a light microscope (Nikon, Japan).

2.4. Tube formation assay to measure angiogenesis

Growth factor-reduced Matrigel (50 mL/well; Corning, Bedford, MA) was added to 96-well culture plates and then incubated for 2 h

in a 37 °C incubator. Then, HepG2 or Huh-7 cells (1×10^5) suspended in extracellular matrix were seeded into Matrigel-coated dishes and treated with different doses of eriodictyol (0, 25, 50, and 100 μM) for 24 h. Tube-like structures on Matrigel were photographed using an inverted microscope (Nikon, Japan).

2.5. Western blot analysis

The proteins extracted from tissues and cells were implemented via RIPA (Sangon Biotech, Shanghai, China). Then, the protein samples were exposed to SDS-PAGE and transferred to PVDF membranes (ThermoFisher, MA, USA). After block with non-fat milk (5 %), membranes were incubated with following primary antibodies: *anti*-NLRP3 antibody (1:500; ab214185), *anti*-VEGFA antibody (1:1000; ab51745), *anti*-MMP3 antibody (1:1000; ab52915), *anti*-MMP16 antibody (1: 500; ab73877), *anti*-ASC antibody (1:5000; ab155970), *anti*-caspase-1 antibody (1:1000; ab138483), *anti*-IL-18 antibody (1:100; ab71495), *anti*-IL-1β antibody (1:200; ab9722), and *anti*-GAPDH antibody (1:10,000; ab181602) in dilution buffer overnight at 4 °C. Membranes were then incubated with HRP-conjugated secondary antibodies (1:5000; ab6721) at 25 °C for 2 h. Finally, the protein signals were detected using enhanced chemiluminescence (ECL, Amersham Pharmacia, Piscataway, NJ, USA). All antibodies were purchased from Abcam (Cambridge, MA, USA). Bands were visualized by an Odyssey CLx Imaging System (Biosciences, NJ, USA).

2.6. Cell transfection

NLRP3-overexpressing pENTER plasmid (Vigene Biosciences, Shandong, China) and NLRP3 siRNA (Vigene Biosciences) were generated and transfected into HepG2 cells, respectively. The process of transfection was used by Lipofectamine 3000 (Invitrogen, CA, USA).

2.7. QRT-PCR assay

Total RNA was isolated from tumor tissues or HepG2 cells and purified by TRIzol reagent (Invitrogen). The reversed transcription was conducted with an RT-PCR kit (Invitrogen), and qRT-PCR was conducted on AB7300 thermo-recycler (Applied Biosystems, CA, USA) using SYBR Green (Applied Biosystems). GAPDH was used as an internal reference. The relative quantification of gene expression was calculated by the $2^{-\Delta\Delta Ct}$ method. Primer sequences were listed as follows:

NLRP3:

Forward: 5'-TTCACCAAGGTCGCACCT G-3'; reverse: 5'-AACTGAACGTTGCAACTTAC-3'.

ASC:

Forward: 5'-CATTGCAATGCTACGCGTG-3'; reverse: 5'-CGGACTCGACATGCTAACT-3'.

Caspase-1:

Forward: 5'-TGCCTGTTCCTGTGATGTGG-3'; reverse: 5'-TGTCCTGGGAAGAGGTAGAAACATC-3'.

IL-18:

Forward: 5'-TGCTACTGAGCTAGCAAC-3'; reverse: 5'-CATTCAGCTGACGGCTGACT-3'

IL-1β:

Forward: 5'-GGACTGACAATGCTGGCAG-3'; reverse: 5'-GGTCGTAATGCTACCGATC-3'

2.8. Tumor xenograft assay to determine tumor growth

The 5-week-old BALB/C nude mice were used to establish a xenograft model. HepG2 cells (1×10^6) transfected with NLRP3-overexpressing pENTER or not were subcutaneously inoculated into the either side of the posterior flank of mice. Fifteen nude mice were included and their tumor growth was examined during the following 30 days. Mice were randomly divided into three groups: control group (tumor-bearing mice were intragastrically administered with equal volume saline), eriodictyol group (tumor-bearing mice were intragastrically administered with 100 mg/kg eriodictyol per day) [23] and eriodictyol + NLRP3 group (nude mice were subcutaneously inoculated with NLRP3-overexpressing-HepG2 cells, with five mice in each group and intragastrically administered with 100 mg/kg eriodictyol). Mice body weight and tumor size were measured every 5 days. All mice were sacrificed on day 30 by an overdose of 100 mg/kg pentobarbital sodium via intravenous injection. Then the dissected tumors were weighted, and tumor and liver tissues were collected for histological analysis and further experiments. The mice experiment was approved by the Animal Ethics Committee of the Third Xiangya Hospital, Central South University.

2.9. Hematoxylin and eosin (HE) staining

Tumor and liver tissues were fixed with 4 % paraformaldehyde for 24 h and then embedded in paraffin. The tissue samples were sectioned at 5 μm thickness and stained with hematoxylin (Beyotime) for 10 min and eosin (Beyotime) for 1 min.

2.10. Immunohistochemistry (IHC)

The paraffin-embedded tumor samples were sectioned at 5 μm thickness. After antigen retrieval, the endogenous peroxidase was blocked with hydrogen peroxide (3 %) for 20 min. The sections were sealed with normal goat serum (5 %) for 30 min and then incubated with primary antibodies, including NLRP3 (ab214185, Abcam), VEGFA (ab51745, Abcam), MMP3 (ab52915, Abcam), and MMP16 (ab73877, Abcam) for 12 h at 4 °C. Then, sections were incubated with secondary antibodies for 60 min at 37 °C and stained with DAB. Finally, sections were counterstained with hematoxylin for 20 s, and images were observed under a light microscope (400× magnification, Nikon, Japan).

2.11. ELISA

Serum of mice was collected and the levels of AST and ALT were measured using Mouse AST ELISA kit (ab263882, Abcam) and Mouse ALT ELISA kit (ab282882, Abcam). The absorbance at 450 nm was read with a microplate reader (Bio-Rad).

2.12. Statistical analysis

All experiments were independently repeated for three times. All data from ≥3 independent experiments were expressed as mean ± standard deviation (SD). Differences between groups were calculated by student *t*-test, and differences among groups were calculated by one-way ANOVA with Tukey's post-hoc test. Statistical analyses were performed using SPSS 20.0 software. $*p < 0.05$ was regarded as statistically significant.

3. Results

3.1. Eriodictyol inhibited cell viability of HCC cells

To observe the effects of eriodictyol on HCC cells, HepG2 and Huh-7 cells were cultured with different doses of eriodictyol (0, 12.5, 25, 50, 100, 200, 400, or 800 μM). The 2D and 3D structure of eriodictyol were shown in Fig. 1A and B. Compared with eriodictyol (0 μM) group, the viability of HepG2 cells was dramatically suppressed by eriodictyol (25, 50, 100, 200, 400, and 800 μM) with IC_{50} of 45.63 μM (Fig. 1C; N = 3, $p < 0.05$). Compared with eriodictyol (0 μM) group, the viability of Huh-7 cells was remarkably inhibited by eriodictyol (50, 100, 200, 400, and 800 μM) with IC_{50} of 78.26 μM (Fig. 1D; N = 3, $p < 0.05$). Based on the result above, doses of eriodictyol, 0, 25, 50, and 100 μM, were chosen for the following experiment.

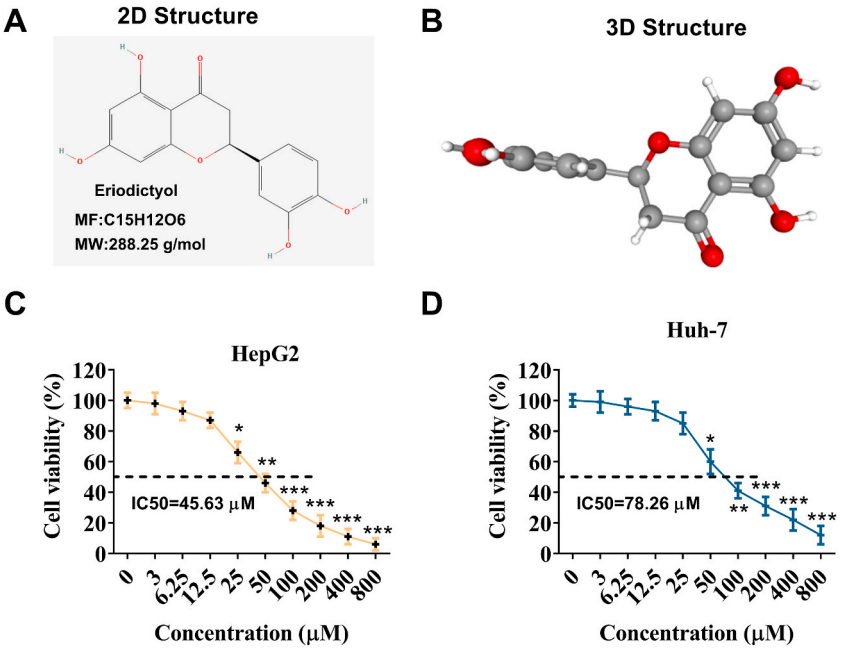

Fig. 1. Effect of Eriodictyol on the viability of HepG2 and Huh-7 cells. (A) The 2D structure of eriodictyol; (B) the 3D structure of eriodictyol; (C, D) HepG2 and Huh-7 cell lines were cultured with different doses of eriodictyol (0, 12.5, 25, 50, 100, 200, 400, or 800 μM) for 2 days, and cell viability was examined by using the CCK-8 assay. $*p < 0.05$, $**p < 0.01$ and $***p < 0.001$, compared with 0 μM group.

3.2. Eriodictyol repressed the motility of HCC cells

Since EMT was involved in cancer invasion and metastasis, we treated HepG2 and Huh-7 cells with different doses of eriodictyol (0, 25, 50, and 100 μM) to observe whether eriodictyol can affect the invasion and metastasis of HepG2 and Huh-7 cells. Compared with eriodictyol (0 μM) group, eriodictyol (25, 50, 100 μM) dramatically reduced the number of invasive HepG2 cells (Fig. 2A and B; $N = 3$, $p < 0.05$) and tube formation of HepG2 cells (Fig. 2C and D; $N = 3$, $p < 0.05$). Compared with eriodictyol (0 μM) group, eriodictyol (50, 100 μM) remarkably reduced the number of invasive Huh-7 cells (Fig. 2A and B) and tube formation of Huh-7 cells (Fig. 2C and D). Images of HCC cells photographed in the light field were shown in Fig. 2E. Furthermore, western blotting confirmed that eriodictyol significantly reduced the levels of metastasis-related genes MMP3, MMP16, and angiogenesis regulator VEGFA in HepG2 (eriodictyol

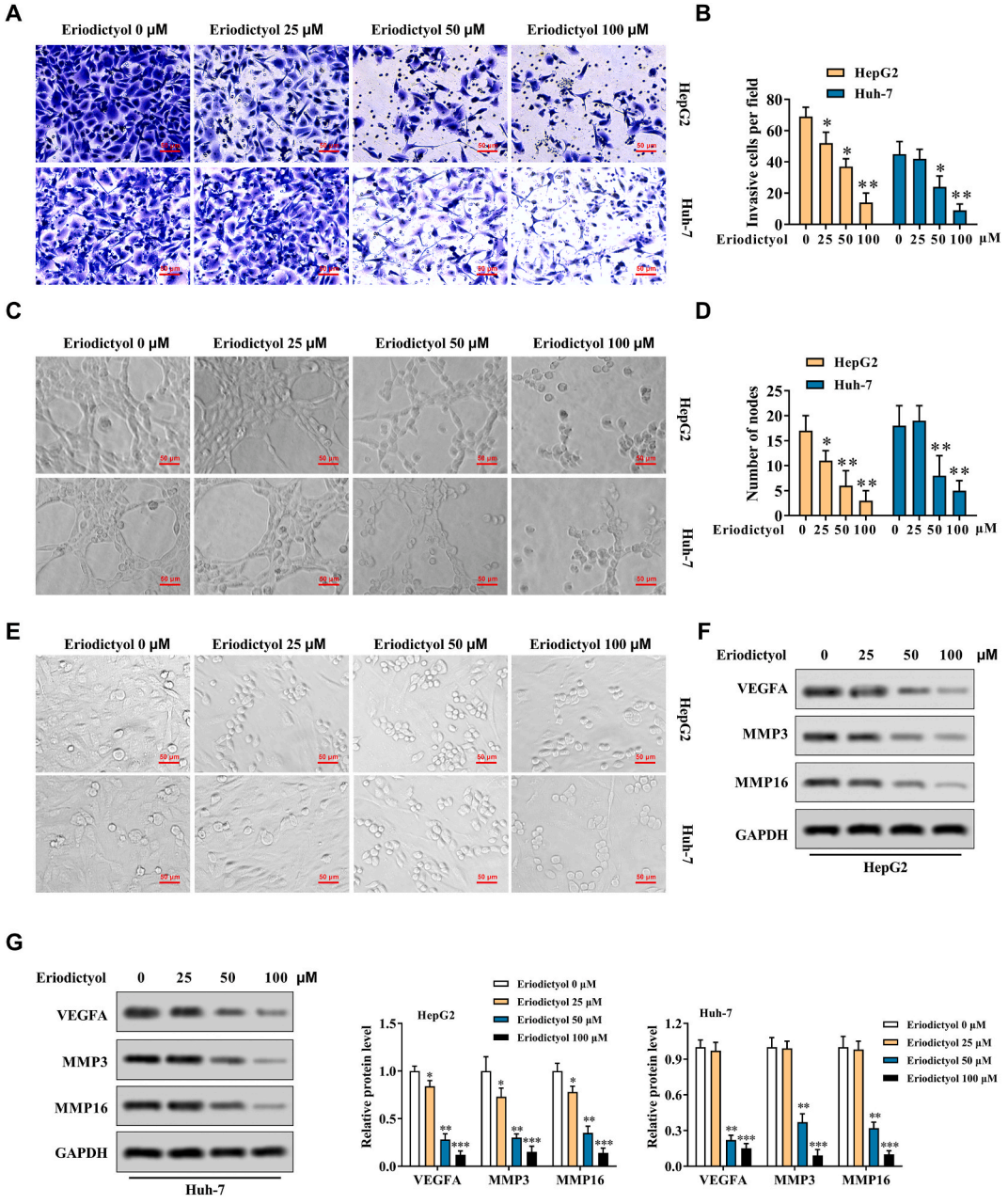

Fig. 2. Effect of Eriodictyol on the motility and EMT in HepG2 and Huh-7 cells. After HepG2 and Huh-7 cells were cultured with different doses of eriodictyol (0, 25, 50, or 100 μM) for 2 days, (A, B) the invasion of HepG2 and Huh-7 cells was assessed by transwell assay; (C, D) the formation of HepG2 and Huh-7 tubes was detected by tube formation assay; (E) images were photographed in the light field; (F, G) expression of VEGFA, MMP3 and MMP16 were assessed by Western blot. *$p < 0.05$, **$p < 0.01$ and ***$p < 0.001$, compared with 0 μM group.

of 25, 50, 100 μM) and Huh-7 cells (eriodictyol of 50, 100 μM) than eriodictyol (0 μM) group (Fig. 2F and G; N = 3, $p < 0.05$). Therefore, eriodictyol repressed the motility, metastasis and tube formation of HepG2 and Huh-7 cells.

3.3. Eriodictyol repressed NLRP3 inflammasome activation in HCC cells

Compared with eriodictyol (0 μM) group, NLRP3 expression was significantly declined by eriodictyol in HepG2 (eriodictyol of 25, 50, 100 μM) and Huh-7 cells (eriodictyol of 50, 100 μM) (Fig. 3A; N = 3, $p < 0.05$). In addition, compared with eriodictyol (0 μM) group, eriodictyol treatment reduced the protein levels of NLRP3 inflammasome-related proteins (ASC, caspase-1, IL-18, and IL-1β) in HepG2 and Huh-7 cells (Fig. 3B, C, 3D; N = 3, $p < 0.05$). These findings suggested that eriodictyol could repress NLRP3 inflammasome activation.

3.4. Upregulation of NLRP3 neutralized the anti-metastatic effects of eriodictyol in vitro

Next, we investigated whether eriodictyol suppressed cell motility, metastasis and tube formation by downregulating NLRP3 in HepG2 cells. Firstly, HepG2 cells were divided into control group (HepG2 cells treated with 100 μM PBS), 100 μM eriodictyol group, NLRP3-overexpressing + 100 μM eriodictyol group, and NLRP3-silencing + 100 μM eriodictyol group. Compared with control group, eriodictyol significantly down-regulated NLRP3 mRNA and protein levels, and NLRP3-overexpressing reversed the inhibition effect of eriodictyol on NLRP3 mRNA and protein levels, whereas NLRP3-silencing + eriodictyol further down-regulated NLRP3 level (Fig. 4A and B; N = 3, $p < 0.05$). Moreover, compared with control group, eriodictyol significantly repressed cell invasion, tube formation and metastasis-related genes MMP3, MMP16, and angiogenesis regulator VEGFA in HepG2 (Fig. 4C, D, 4E and 4F; N = 3, $p < 0.05$). Whereas overexpression of NLRP3 neutralized the inhibitory effect of eriodictyol on cell invasion, tube formation and metastasis-related genes MMP3, MMP16, and angiogenesis regulator VEGFA (Fig. 4C, D, 4E and 4F; N = 3, $p < 0.05$). While silencing of NLRP3 aggravated the inhibitory effect of eriodictyol on cell invasion, tube formation, and metastasis-related genes MMP3, MMP16, and angiogenesis regulator VEGFA in HepG2 cells (Fig. 4C, D, 4E and 4F; N = 3, $p < 0.05$). Hence, these findings indicated that eriodictyol might inhibit HCC cell motility, metastasis and tube formation by downregulating NLRP3.

3.5. Upregulation of NLRP3 neutralized the anti-tumor effects of eriodictyol in vivo

As shown in Fig. 5A–F, compared with control group, eriodictyol treatment significantly reduced tumor volume, tumor weight and liver histopathological damage (N = 5, $p < 0.05$). Whereas overexpression of NLRP3 significantly neutralized the restraint of eriodictyol on tumor volume and tumor weight, and weakened the amelioration of eriodictyol on liver damage, which indicated that upregulation of NLRP3 accelerated the growth of HCC tumor (N = 5, $p < 0.05$). In addition, compared with control group, eriodictyol suppressed the expression of NLRP3, metastasis-related genes MMP3 and MMP16, angiogenesis regulator VEGFA, whereas overexpression of NLRP3 reversed the suppression of eriodictyol on NLRP3, metastasis-related genes MMP3 and MMP16, angiogenesis regulator VEGFA expression (Fig. 5G and H; N = 5, $p < 0.05$). In addition, compared with control group, eriodictyol treatment significantly reduced the levels of liver damage markers AST and ALT in serum, whereas NLRP3 overexpression reversed the

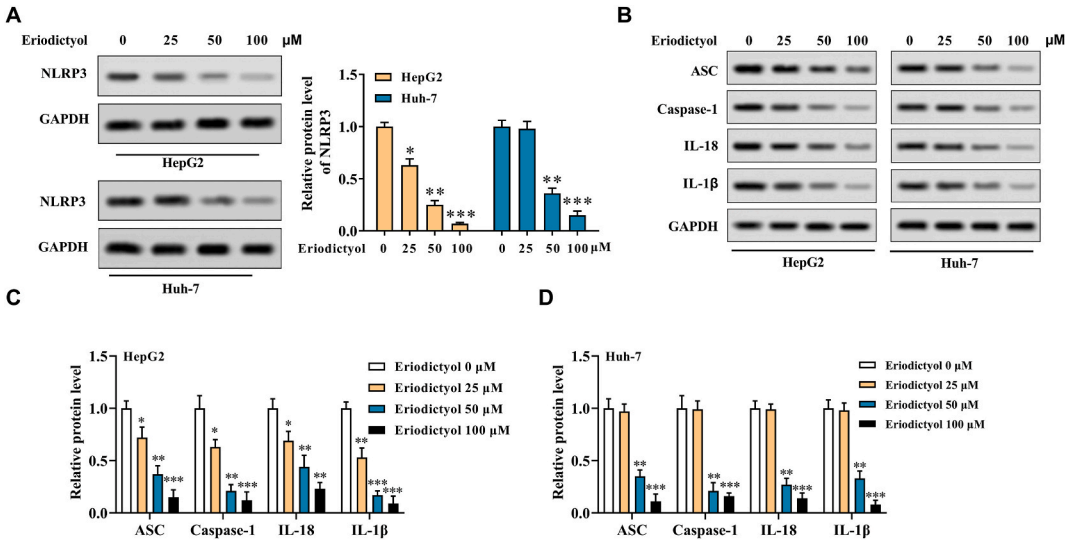

Fig. 3. Eriodictyol repressed NLRP3 inflammasome activation in HCC cells. After HepG2 and Huh-7 cells were cultured with different doses of eriodictyol (0, 25, 50, or 100 μM) for 2 days, (A) the NLRP3 expression was assessed by Western blot; (B, C, D) protein levels of ASC, caspase-1, IL-18, and IL-1β in HepG2 and Huh-7 cells were measured by Western blot. *$p < 0.05$, **$p < 0.01$ and ***$p < 0.001$, compared with 0 μM group.

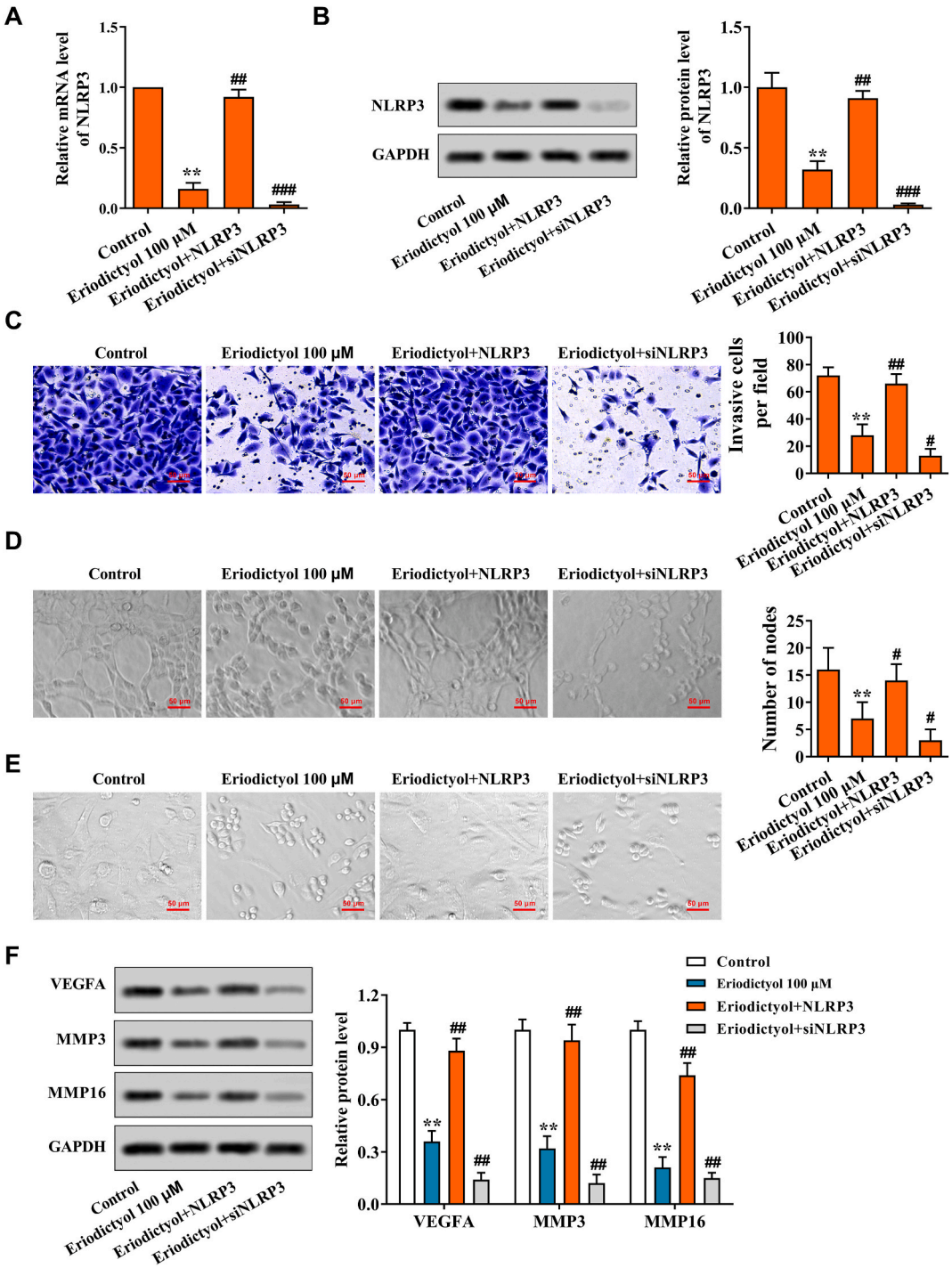

Fig. 4. Upregulation of NLRP3 neutralized the anti-metastatic effects of eriodictyol *in vitro*. HepG2 cells were divided into control group, 100 μM eriodictyol group, NLRP3-overexpressing +100 μM eriodictyol group, and NLRP3-silencing +100 μM eriodictyol group, (A) NLRP3 mRNA level was detected by RT-PCR; (B) NLRP3 protein level was evaluated by Western blot; (C) the invasion of HepG2 cells was assessed by transwell assay; (D) the formation of HepG2 tubes was detected by tube formation assay; (E) images were photographed in the light field; (F) expression of VEGFA, MMP3 and MMP16 were detected by Western blot. (*$p < 0.05$ and **$p < 0.01$ vs control group, #$p < 0.05$ and ##$p < 0.01$ vs eriodictyol group).

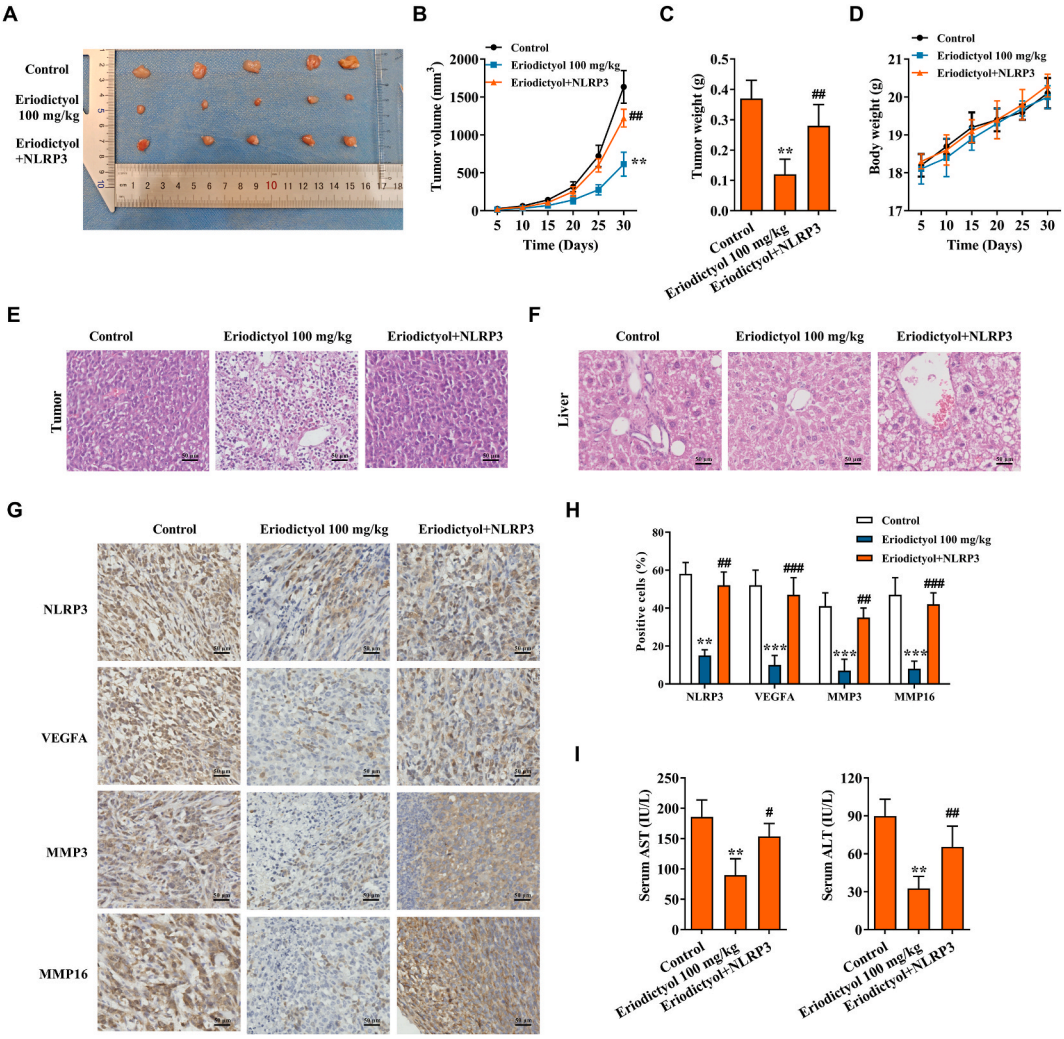

Fig. 5. NLRP3 overexpression abrogated the anti-tumor effects of eriodictyol *in vivo*. (A) Images of subcutaneous tumors of control, eriodictyol, and eriodictyol + NLRP3 group mice (n = 5/per group). (B) The growth curve of xenograft tumor in the control, eriodictyol, and eriodictyol + NLRP3 groups. (C) Tumor weight in the control, eriodictyol, and eriodictyol + NLRP3 groups. (D) The growth curve of body weight of mice in the control, eriodictyol, and eriodictyol + NLRP3 groups. (E, F) Pathological damage of the tumor and liver was detected by H&E staining. (G) Immunohistochemical staining of NLRP3, VEGFA, MMP3, and MMP16 in tumor tissues. (H) Positive staining rates of NLRP3, VEGFA, MMP3, and MMP16. (I) The levels of AST and ALT were determined by ELISA. (**$p < 0.01$ vs control group, ##$p < 0.01$ vs eriodictyol group).

suppression of eriodictyol on AST and ALT levels (Fig. 5I; N = 5, p < 0.05).

3.6. *Upregulation of NLRP3 neutralized the inhibitory effect of eriodictyol on NLRP3 inflammasome*

Since we found that eriodictyol treatment reduced NLRP3 expression, we speculated the anti-tumor effect of eriodictyol was related with NLRP3 inflammasome inactivation. As expected, compared with control group, the eriodictyol treatment also significantly reduced the mRNA and protein levels of NLRP3 inflammasome-related proteins, ASC, caspase-1, IL-18, and IL-1β (Fig. 6A–E; N = 5, p < 0.05). Conversely, NLRP3 overexpression attenuated the inhibitory effect of eriodictyol on the expression of ASC, caspase-1, IL-18, and IL-1β (Fig. 6A–E; N = 5, p < 0.05). Taken together, these above results suggested that eriodictyol could suppress tumor growth and metastasis by inhibiting NLRP3 and further inhibiting NLRP3 inflammasome activation. The idea of this manuscript was summarized by **Graphical abstract** (Fig. 7).

4. Discussion

Tumor metastasis and recurrence are the leading causes of the poor prognosis of HCC patients [24–26]. Therefore, identifying metastasis-associated factors, elucidating the mechanism underlying HCC metastasis, and developing effective anti-cancer drugs are

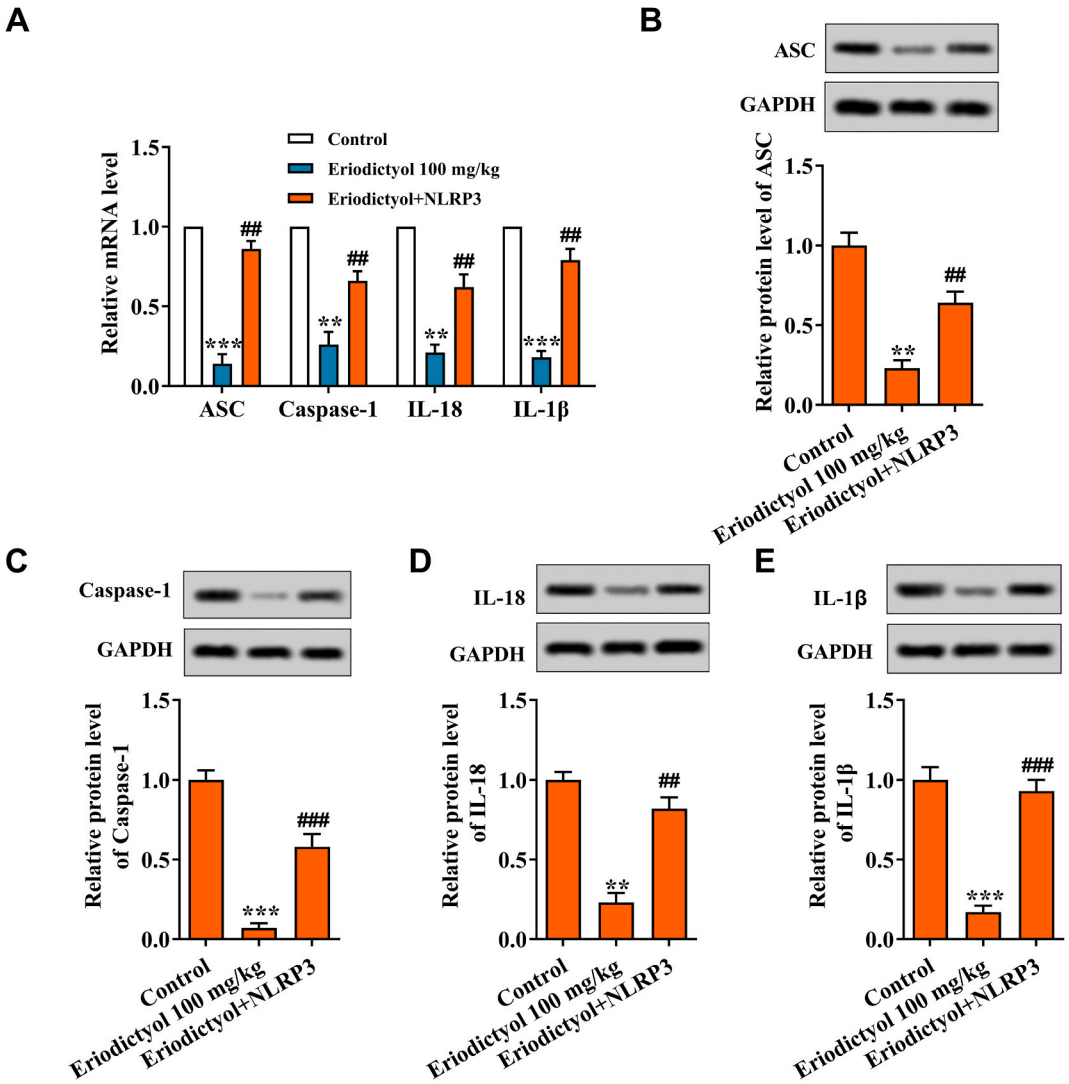

Fig. 6. Upregulation of NLRP3 neutralized the inhibitory effect of eriodictyol on NLRP3 inflammasome. (A) The mRNA levels of ASC, caspase-1, IL-18, and IL-1β were measured by RT-qPCR. The protein levels of ASC (B), caspase-1 (C), IL-18 (D), and IL-1β (E) were measured by western blotting. (**$p < 0.01$ vs control group, ##$p < 0.01$ vs eriodictyol group).

essential for the diagnosis, supervision, and treatment of HCC patients. In this study, eriodictyol exerted anti-metastatic function by repressing the HCC cells viability, invasion, tube formation and EMT-related genes MMP3 and MMP16 expressions, angiogenesis regulator VEGFA expression *in vitro*. Meanwhile, compared with control group, NLRP3 overexpression reversed the anti-metastatic effects of 100 μM eriodictyol on HCC cells invasion, tube formation, metastasis-related genes MMP3 and MMP16, and angiogenesis regulator VEGFA expressions, whereas NLRP3 knockdown enhanced the anti-metastatic effects of 100 μM eriodictyol on HCC cells. In addition, *in vivo* assays in a xenograft model confirmed eriodictyol significantly reduced the tumor growth, liver damage, inhibited the activation of NLRP3 inflammasome, and improved liver function, whereas NLRP3 overexpressing neutralized the anti-tumor effects of eriodictyol and degraded liver function. The present study provides evidence that eriodictyol could play an anti-cancer role in HCC by downregulating NLRP3 expression.

In the past few years, despite the unprecedented development of therapeutic strategies for HCC, large numbers of HCC patients still suffer from the predicament of poor prognosis or serious adverse effects [27,28]. This is partly due to ineffective treatment, therapeutic resistance, or drug toxicity. Therefore, it is urgent to develop effective and noncytotoxic drugs for HCC treatment. Natural herbs play an irreplaceable role in the development of antitumor drug relying on their high efficiency and limited toxicity [4]. Accumulated evidence found that the metastasis of HCC cells could be inhibited by some flavonoids, including luteoloside [21], puerarin [29], scutellarin [30], and vitexin [31]. As a flavone subclass of flavonoids, eriodictyol showed anti-inflammatory and anti-oxidant effects by regulating Akt- and NF-κB related pathways [32–34]. However, study focus on the anti-cancer effect of eriodictyol on HCC and its underlying mechanism is not found. In this study, eriodictyol showed a metastasis inhibition effect on HCC through suppressing HCC

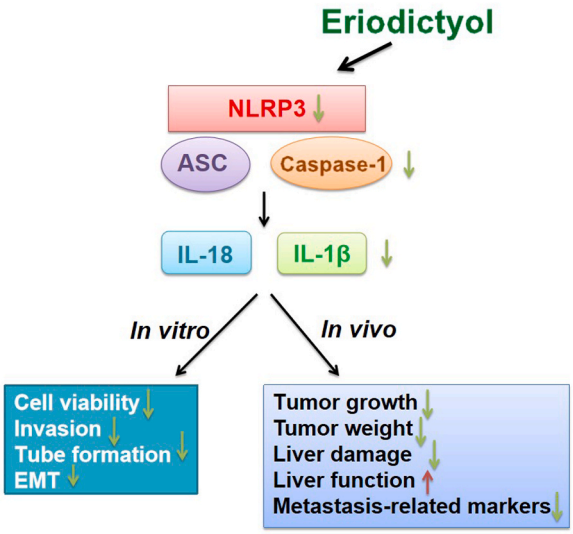

Fig. 7. Graphical abstract. Eriodictyol repressed HCC cell viability, invasion, EMT *in vitro*, and inhibited tumor growth and liver damage and improved liver function *in vivo* via NLRP3 inflammasom.

cell invasion, tube formation, and EMT.

Angiogenesis is a complex process, including endothelial cell proliferation, invasion, and new tube formation, which is crucial in tumor metastasis progression [35]. VEGFA is a key regulator of angiogenesis, and VEGFA knockdown could inhibit angiogenesis [36]. This study demonstrated that eriodictyol showed suppression effects on tube formation and expression of VEGFA in HCC cells. As an indispensable role in the poor prognosis of HCC, EMT activation leads to drug resistance, recurrence, and metastasis to distant organs in HCC [37]. EMT plays a leading role in the early steps of metastasis, which makes tumor cells lose apical-basal polarity, cell-cell contacts, and basement-membrane, and achieve the transformation from epithelial-like phenotype to mesenchymal-like phenotype [38]. These transformations endow the tumor cells with the ability to spread to surrounding or distant tissues, subsequently leading to recurrence or metastasis. In malignancies, MMPs play significant roles in the EMT process and contribute to promoting EMT via invasion and metastasis [38]. We demonstrated that eriodictyol could inhibit the expression of MMP3 and MMP16. Tumor metastasis and recurrence are the main causes of poor prognosis and cancer death in HCC patients [39]. Thus, attention should be focused on the identification of metastasis-associated factors to repress metastasis in HCC.

Accumulated evidence showed that NLRP3 could be regulated by some natural herbs. For instance, GEN-27, a derivative of genistein, played an anti-inflammatory role in repressing NLRP3 inflammasome activation [40]. Berberine repressed NLRP3 inflammasome pathway in triple-negative breast cancer [41]. In HCC, anisodamine could restrain HCC cell growth and promote HCC cell apoptosis by blocking NLRP3 inflammasome activation [20]. Similarly, luteoloside exhibited suppressive effects on HCC cell growth and metastasis via suppression of NLRP3 inflammasome [21]. Considering the previous reports and the findings in this study, we speculated that eriodictyol exhibited inhibitory effects on HCC cell metastasis by downregulating NLRP3 expression. In this study, we found that along with the increase of NLRP3 expression, the inhibitory effects of eriodictyol on cell motility were significantly abrogated in HepG2 cells. Besides, NLRP3 overexpression reversed the inhibition effects of eriodictyol on tumor growth and metastasis in a xenograft model. Conversely, along with the decrease of NLRP3 expression, the inhibitory effects of eriodictyol on cell motility were significantly enhanced in HepG2 cells. NLRP3 inflammasome, includes NLRP3, ASC, caspase-1, IL-1β, and IL-18 proteins, and its activation is involved in the HCC progression [42–44]. This study demonstrated that the inhibitory effects of eriodictyol on NLRP3, ASC, caspase-1, IL-1β, and IL-18 expression were abrogated by NLRP3 overexpression, which suggested that upregulation of NLRP3 neutralized the inhibitory effects of eriodictyol on NLRP3 inflammasome. The above findings suggested that these anti-cancer effects of eriodictyol may be achieved by downregulating NLRP3 signaling.

5. Conclusions

Our study firstly showed that NLRP3 inflammasome inactivation was involved in the inhibition effects of eriodictyol on HCC cells viability, motility, angiogenesis and tumor growth both *in vitro* and *in vivo*. All these findings provided a theoretical foundation for the possibility of eriodictyol used as a promising drug for HCC therapy. Researchers can focus on eriodictyol and its underlying mechanism NLRP3 inflammasome on HCC in future associated studies. However, there are some limitations in this study. We didn't assess the clinical significance of survival outcomes, metastasis prevention, and overall therapeutic efficacy, as well as long-term toxicity and pharmacokinetic analyses. We will focus on the clinical significance in further studies. In addition, we didn't consider positive drug controls when we determine the concentration of eriodictyol on HCC viability, invasion and tube formation *in vitro*.

Data availability statement

The data used to support the findings of this study are available from the corresponding author upon request.

Funding statement

This project has received support from Research Plan of Hunan Provincial Health Commission (B202304088695).

Ethics approval statement

The protocol for animal study was followed with the ethical standards of Third Xiangya Hospital, Central South University (LUNSHEN-2020-023).

CRediT authorship contribution statement

Wei Huang: Investigation, Data curation, Conceptualization. **Chenyang Wang:** Software, Resources. **Hui Zhang:** Methodology, Investigation, Formal analysis.

Declaration of competing interest

The authors declare that they have no known competing financial interests or personal relationships that could have appeared to influence the work reported in this paper.

Appendix A. Supplementary data

Supplementary data to this article can be found online at https://doi.org/10.1016/j.heliyon.2024.e24401.

References

[1] A. Villanueva, Hepatocellular carcinoma, N. Engl. J. Med. 380 (15) (2019) 1450–1462.
[2] H.I. Yang, et al., Nomograms for risk of hepatocellular carcinoma in patients with chronic hepatitis B virus infection, J. Clin. Oncol. 28 (14) (2010) 2437–2444.
[3] Y. Kawano, et al., Prognosis of patients with intrahepatic recurrence after hepatic resection for hepatocellular carcinoma: a retrospective study, Eur. J. Surg. Oncol. 35 (2) (2009) 174–179.
[4] T. Efferth, et al., Collateral sensitivity of natural products in drug-resistant cancer cells, Biotechnol. Adv. 38 (2020) 107342.
[5] K. Minato, et al., Lemon flavonoid, eriocitrin, suppresses exercise-induced oxidative damage in rat liver, Life Sci. 72 (14) (2003) 1609–1616.
[6] B. Zeng, et al., Phenolic compounds from clinopodium chinense (benth.) O. Kuntze and their inhibitory effects on alpha-glucosidase and vascular endothelial cells injury, Chem. Biodivers. 13 (5) (2016) 596–601.
[7] A. Islam, et al., The pharmacological and biological roles of eriodictyol, Arch Pharm. Res. (Seoul) 43 (6) (2020) 582–592.
[8] P. He, et al., Eriodictyol attenuates LPS-induced neuroinflammation, amyloidogenesis, and cognitive impairments via the inhibition of NF-kappaB in male C57bl/6J mice and BV2 microglial cells, J. Agric. Food Chem. 66 (39) (2018) 10205–10214.
[9] E.Y. Kwon, M.S. Choi, Dietary eriodictyol alleviates adiposity, hepatic steatosis, insulin resistance, and inflammation in diet-induced obese mice, Int. J. Mol. Sci. 20 (5) (2019).
[10] P. Lv, et al., Eriodictyol inhibits high glucose-induced oxidative stress and inflammation in retinal ganglial cells, J. Cell. Biochem. 120 (4) (2019) 5644–5651.
[11] L. Tang, et al., Eriodictyol inhibits the growth of CNE1 human nasopharyngeal cancer growth by targeting MEK/ERK signalling pathway, inducing cellular autophagy and inhibition of cell migration and invasion, J BUON 25 (5) (2020) 2389–2394.
[12] Y. Zhang, R. Zhang, H. Ni, Eriodictyol exerts potent anticancer activity against A549 human lung cancer cell line by inducing mitochondrial-mediated apoptosis, G2/M cell cycle arrest and inhibition of m-TOR/PI3K/Akt signalling pathway, Arch. Med. Sci. 16 (2) (2020) 446–452.
[13] W. Li, et al., Eriodictyol inhibits proliferation, metastasis and induces apoptosis of glioma cells via PI3K/Akt/NF-kappaB signaling pathway, Front. Pharmacol. 11 (2020) 114.
[14] K. Schroder, J. Tschopp, The inflammasomes, Cell 140 (6) (2010) 821–832.
[15] I.S. Afonina, et al., Limiting inflammation-the negative regulation of NF-kappaB and the NLRP3 inflammasome, Nat. Immunol. 18 (8) (2017) 861–869.
[16] X. Shao, Z. Lei, C. Zhou, NLRP3 promotes colorectal cancer cell proliferation and metastasis via regulating epithelial mesenchymal transformation, Anti Cancer Agents Med. Chem. 20 (7) (2020) 820–827.
[17] N. Ershaid, et al., NLRP3 inflammasome in fibroblasts links tissue damage with inflammation in breast cancer progression and metastasis, Nat. Commun. 10 (1) (2019) 4375.
[18] Y. Xue, et al., Correlation between the NLRP3 inflammasome and the prognosis of patients with LSCC, Front. Oncol. 9 (2019) 588.
[19] H.E. Lee, et al., Inhibition of NLRP3 inflammasome in tumor microenvironment leads to suppression of metastatic potential of cancer cells, Sci. Rep. 9 (1) (2019) 12277.
[20] P. Li, Y. Liu, Q. He, Anisodamine suppressed the growth of hepatocellular carcinoma cells, induced apoptosis and regulated the levels of inflammatory factors by inhibiting NLRP3 inflammasome activation, Drug Des. Dev. Ther. 14 (2020) 1609–1620.
[21] S.H. Fan, et al., Luteoloside suppresses proliferation and metastasis of hepatocellular carcinoma cells by inhibition of NLRP3 inflammasome, PLoS One 9 (2) (2014) e89961.
[22] W. Chen, et al., Downregulation of IRAK1 prevents the malignant behavior of hepatocellular carcinoma cells by blocking activation of the MAPKs/NLRP3/IL-1beta pathway, OncoTargets Ther. 13 (2020) 12787–12796.
[23] W. Li, et al., Eriodictyol inhibits proliferation, metastasis and induces apoptosis of glioma cells via PI3K/Akt/NF-κB signaling pathway, Front. Pharmacol. (2020) 11.
[24] A.G. Singal, H.B. El-Serag, Hepatocellular carcinoma from epidemiology to prevention: translating knowledge into practice, Clin. Gastroenterol. Hepatol. 13 (12) (2015) 2140–2151.

[25] H.B. El-Serag, K.L. Rudolph, Hepatocellular carcinoma: epidemiology and molecular carcinogenesis, Gastroenterology 132 (7) (2007) 2557–2576.
[26] D. Graf, et al., Multimodal treatment of hepatocellular carcinoma, Eur. J. Intern. Med. 25 (5) (2014) 430–437.
[27] J.R. Desai, et al., Systemic therapy for advanced hepatocellular carcinoma: an update, J. Gastrointest. Oncol. 8 (2) (2017) 243–255.
[28] T.M. Cui, et al., Adverse effects of immune-checkpoint inhibitors in hepatocellular carcinoma, OncoTargets Ther. 13 (2020) 11725–11740.
[29] Y. Zhou, et al., Puerarin inhibits hepatocellular carcinoma invasion and metastasis through miR-21-mediated PTEN/AKT signaling to suppress the epithelial-mesenchymal transition, Braz. J. Med. Biol. Res. 53 (4) (2020) e8882.
[30] Y. Ke, et al., Scutellarin suppresses migration and invasion of human hepatocellular carcinoma by inhibiting the STAT3/Girdin/Akt activity, Biochem. Biophys. Res. Commun. 483 (1) (2017) 509–515.
[31] J.H. Lee, et al., Vitexin abrogates invasion and survival of hepatocellular carcinoma cells through targeting STAT3 signaling pathway, Biochimie 175 (2020) 58–68.
[32] G. Xie, et al., Eriodictyol attenuates arsenic trioxide-induced liver injury by activation of Nrf2, Oncotarget 8 (40) (2017) 68668–68674.
[33] Y. Liu, X. Yan, Eriodictyol inhibits survival and inflammatory responses and promotes apoptosis in rheumatoid arthritis fibroblast-like synoviocytes through AKT/FOXO1 signaling, J. Cell. Biochem. 120 (9) (2019) 14628–14635.
[34] Y. Wang, et al., Eriodictyol inhibits IL-1beta-induced inflammatory response in human osteoarthritis chondrocytes, Biomed. Pharmacother. 107 (2018) 1128–1134.
[35] M. Rajabi, S.A. Mousa, The role of angiogenesis in cancer treatment, Biomedicines 5 (2) (2017).
[36] K.S. Siveen, et al., Vascular endothelial growth factor (VEGF) signaling in tumour vascularization: potential and challenges, Curr. Vasc. Pharmacol. 15 (4) (2017) 339–351.
[37] G. Giannelli, et al., Role of epithelial to mesenchymal transition in hepatocellular carcinoma, J. Hepatol. 65 (4) (2016) 798–808.
[38] B.N. Smith, N.A. Bhowmick, Role of EMT in metastasis and therapy resistance, J. Clin. Med. 5 (2) (2016).
[39] Y.C. Liu, C.T. Yeh, K.H. Lin, Cancer stem cell functions in hepatocellular carcinoma and comprehensive therapeutic strategies, Cells 9 (6) (2020).
[40] M. Hu, et al., GEN-27 exhibits anti-inflammatory effects by suppressing the activation of NLRP3 inflammasome and NF-kappaB pathway, Cell Biol. Int. 43 (10) (2019) 1184–1192.
[41] M. Yao, et al., Berberine inhibits NLRP3 Inflammasome pathway in human triple-negative breast cancer MDA-MB-231 cell, BMC Compl. Alternative Med. 19 (1) (2019) 216.
[42] Q. Wei, et al., E2-Induced activation of the NLRP3 inflammasome triggers pyroptosis and inhibits autophagy in HCC cells, Oncol. Res. 27 (7) (2019) 827–834.
[43] Q. Wei, et al., Estrogen suppresses hepatocellular carcinoma cells through ERbeta-mediated upregulation of the NLRP3 inflammasome, Lab. Invest. 95 (7) (2015) 804–816.
[44] B.Z. Shao, et al., NLRP3 inflammasome and its inhibitors: a review, Front. Pharmacol. 6 (2015) 262.